Acta Pharmaceutica Sinica B 2025;15(6):3092−3106

Chinese Pharmaceutical Association
Institute of Materia Medica, Chinese Academy of Medical Sciences

Acta Pharmaceutica Sinica B

www.elsevier.com/locate/apsb
www.sciencedirect.com

ORIGINAL ARTICLE

ALKBH3-regulated m^{1}A of ALDOA potentiates glycolysis and doxorubicin resistance of triple negative breast cancer cells

Yuhua Deng[a,c,†], Zhiyan Chen[a,b,†], Peixian Chen[a], Yaming Xiong[c], Chuling Zhang[c], Qiuyuan Wu[a,b], Huiqi Huang[a], Shuqing Yang[a], Kun Zhang[a], Tiancheng He[a], Wei Li[a], Guolin Ye[a], Wei Luo[c], Hongsheng Wang[d,*], Dan Zhou[a,b,*]

[a]*Department of Breast Surgery, the First People's Hospital of Foshan, Foshan 528100, China*
[b]*Guangdong Medical University, Zhanjiang 524000, China*
[c]*Institute of Translational Medicine Research, the First People's Hospital of Foshan, Foshan 528100, China*
[d]*Guangdong Provincial Key Laboratory of Chiral Molecule and Drug Discovery, State Key Laboratory of Anti-Infective Drug Discovery and Development, School of Pharmaceutical Sciences, Sun Yat-sen University, Guangzhou 510006, China*

Received 20 August 2024; received in revised form 21 November 2024; accepted 20 December 2024

KEY WORDS

Glycolysis;
Chemoresistance;
ALKBH3;
m^{1}A;
ALDOA;
Stability;
TNBC;
3′UTR

Abstract Chemotherapy is currently the mainstay of systemic management for triple-negative breast cancer (TNBC), but chemoresistance significantly impacts patient outcomes. Our research indicates that Doxorubicin (Dox)-resistant TNBC cells exhibit increased glycolysis and ATP generation compared to their parental cells, with this metabolic shift contributing to chemoresistance. We discovered that ALKBH3, an m^{1}A demethylase enzyme, is crucial in regulating the enhanced glycolysis in Dox-resistant TNBC cells. Knocking down ALKBH3 reduced ATP generation, glucose consumption, and lactate production, implicating its involvement in mediating glycolysis. Further investigation revealed that aldolase A (ALDOA), a key enzyme in glycolysis, is a downstream target of ALKBH3. ALKBH3 regulates *ALDOA* mRNA stability through m^{1}A demethylation at the 3′-untranslated region (3′UTR). This methylation negatively affects *ALDOA* mRNA stability by recruiting the YTHDF2/PAN2−PAN3 complex, leading to mRNA degradation. The ALKBH3/ALDOA axis promotes Dox resistance both *in vitro* and *in vivo*. Clinical analysis demonstrated that ALKBH3 and ALDOA are upregulated in breast

*Corresponding authors.
E-mail addresses: zhoudanms@hotmail.com (Dan Zhou), whongsh@mail.sysu.edu.cn (Hongsheng Wang).
[†]These authors made equal contributions to this work.
Peer review under the responsibility of Chinese Pharmaceutical Association and Institute of Materia Medica, Chinese Academy of Medical Sciences.

https://doi.org/10.1016/j.apsb.2025.04.018

cancer tissues, and higher expression of these proteins is associated with reduced overall survival in TNBC patients. Our study highlights the role of the ALKBH3/ALDOA axis in contributing to Dox resistance in TNBC cells through regulation of *ALDOA* mRNA stability and glycolysis.

1. Introduction

Triple-negative breast cancer (TNBC), which constitutes approximately 15% of all invasive breast carcinomas, represents a heterogeneous consortium of breast malignancies, distinguished by the absence of estrogen receptors (ERs), progesterone receptors (PRs), and gene amplification of the human epidermal growth factor receptor 2 (HER2)[1]. Consequently, TNBC remains impervious to endocrine therapy and HER2-targeted interventions[2]. Therefore, cytotoxic chemotherapy stands as the current cornerstone of systemic therapy for both early and advanced TNBC[3]. However, recurrence rates remain high, and TNBC lesions frequently acquire resistance against chemotherapeutic agents[3]. Once chemotherapy fails to overcome resistance in TNBC patients, treatment options are severely limited. Thus, chemoresistance represents a major contributor to mortality in patients with TNBC.

The resistant TNBC cells manifest an augmented glycolytic phenotype, wherein glucose uptake and lactate fermentation surge[4]. It has been revealed that targeted silencing of the pivotal enzymes involved in aerobic glycolysis pathway may potentiate the anti-proliferative efficacy of chemotherapeutic agents. For example, metabolic adaptation towards glycolysis supports resistance to neoadjuvant chemotherapy in early TNBCs[5]. Increased expression of lactate dehydrogenase A (LDHA) is identified in paclitaxel-resistant TNBC cells, and the attenuation of LDHA or the employment of LDH inhibitor oxamate both re-sensitize paclitaxel-resistant TNBC cells to paclitaxel[6]. Further, a recent study has revealed that up-regulated aldolase A (ALDOA) expression promotes the proliferation, sphere formation, and radio-resistance of cancer cells[7]. Targeting glucose metabolism can overcome chemoresistance to anticancer chemotherapy in TNBC[8]. Therefore, targeted inhibition of glycolytic enzymes or their regulators might be potential approaches to re-sensitize TNBC cells to chemotherapy.

Epigenetic reprogramming plays a key role in the acquisition of chemoresistant potential of cancer cells[9]. Post-transcriptional RNA modification, known as the epitranscriptome, has garnered considerable attention due to its extensive involvement in tumor progression[10]. It has been reported that alteration of the m^6A modification, the most common epigenetic RNA modification, affected drug efficacy by restructuring multidrug efflux transporters, drug-metabolizing enzymes, and anticancer drug targets[11]. For example, METTL3 m^6A-dependently enhanced translation of *ABCD1*, leading to migration and spheroid formation in clear cell renal cell carcinoma (ccRCC)[12]. N^1-methyladenosine (m^1A) represents a methylation modification of RNA. Although m^1A is less abundant than m^6A, its impact on RNA structure and function exceeds that of m6A due to the additional positive charge introduced at the modified nitrogen[13]. Previous study discovered correlations between various m^1A methyltransferase, demethylases, and cancer prognosis[14]. However, limited information exists concerning the functional roles of m^1A modification in TNBC progression and chemoresistance.

In the present study, we revealed that the significant elevation of glycolysis of doxorubicin (Dox)-resistance of TNBC cells. Further, there is decrease of m^1A levels in Dox-resistant cells, while ALKBH3-deleted cells were more Dox sensitive. Mechanistical investigations showed that ALKBH3 increased the mRNA stability of ALDOA to trigger glycolysis and chemoresistance of TNBC cells.

2. Materials and methods

2.1. Cell line and cell culture

The triple-negative breast cancer cell line MDA-MB-231 and BT-549 were purchased from the American Type Culture Collection (ATCC, VA, USA). These cell lines underwent regular authentication through STR analysis and were checked for mycoplasma contamination. The cells were cultured in Dulbecco's modified Eagle's medium (DMEM) (Invitrogen Life Technologies) supplemented with 10% fetal bovine serum (FBS, Gibco, Carlsbad, CA, USA) and 1% penicillin/streptomycin (Gibco, USA). The cultures were maintained in a 37 °C incubator with 5% CO_2. Doxorubicin-resistant TNBC cells were generated by treating the cells with increasing concentrations of doxorubicin for approximately 6 months according to the previous study[15]. The resulting resistant cells were named MDA-MB-231/Dox and BT-549/Dox, respectively. To maintain the resistance, the cells were reselected with doxorubicin every 3 months or 5−7 passages. Before experiments, the doxorubicin-resistant cells were cultured in full medium without doxorubicin for three days.

2.2. Plasmid, siRNA, and transfection

To construct the ALKBH3 overexpression vector, the full-length sequence of human ALKDH3 was inserted into the pcDNA3.1 vector (Geenseed Biotech, Guangzhou, China). The pcDNA-ALKBH3 R122A and L177A mutations were generated according to the previous study[16]. The primers used for the R122A mutation were as follows: forward 5′-GAG GAC CGG CAT CGC AGA GGA TA-3′ and reverse 5′-AAG TTA TAT CCT CTG CGA TGC CG-3′. The primers for the L177A mutation were as follows: forward 5′-CAA CTC CTT AGC ATG CAA T-3′ and reverse 5′-TTG CGA TAA AGA TTG CAT GCT AA-3′. The lentiviral vector carrying sh-ALKBH3 or sh-NC, along with two assistant vectors, was transiently transfected into HEK293T cells. After 48 h, the viral supernatants were collected, clarified, and concentrated for animal studies. The TNBC cells were stably transfected or infected with puromycin selection. The pcDNA3.1-YTHDF2 and pcDNA3.1-ALDOA vectors were purchased from Sangon Biotech (Shanghai, China) and verified by sequencing. All

transfections were performed using Lipofectamine 2000 (Invitrogen, Carlsbad, CA, USA) following the manufacturer's instructions.

2.3. Cell viability

Cell viability was assessed using the Cell Counting Kit-8 (CCK8) assay (Abcam, MA, USA) according to the manufacturer's instructions. Cells (1×10^3 per well) were seeded in 96-well plates and allowed to adhere for 12 h. Different concentrations of doxorubicin were added to each well for 24 h. At the end of the experiment, CCK-8 solution (10 μL) was added to each well and incubated with cells for 4 h at 37 °C in the dark. The absorbance of each well was measured at 450 nm using the Multiskan FC microplate photometer (Thermo Scientific, CA, USA). The cell proliferation rate was presented as the relative percentage change in absorbance.

2.4. ATP measurement

Intracellular ATP levels were measured using the ATP Assay Kit (S0026, Beyotime, China) following the manufacturer's instructions. Cells were washed three times with cold PBS and immediately lysed on ice. The cell lysates were then centrifuged at 12,000 × *g* and 4 °C for 5 min. Next, 20 μL of the supernatant and 100 μL of the detection working solution were added to each well of a 96-well plate. The mixture was gently mixed and incubated for 5 min. The intracellular ATP level was assessed using the bioluminescence method with a multi-function microreader.

2.5. Glucose consumption and lactate production

Cells were cultured and treated under the indicated conditions. At the end of the experiment, the culture medium was collected to determine the glucose concentration and lactate levels. Glucose and lactate were measured using the Glucose assay kit (Amplite™ Glucose Quantitation Assay kit, AAT Bioquest, Sunnyvale, USA) and the Lactate Assay Kit II (Eton Bioscience Inc., San Diego, CA, USA) according to the manufacturer's instructions, respectively. Glucose consumption was calculated as the difference in glucose concentration between the fresh medium and cell supernatant. Lactate production was determined as the difference in lactate concentration between the cell supernatant and fresh medium. Each level was normalized to the cell number.

2.6. Metabolites measurement

Intracellular glycolytic intermediates (2/3-PGs, PEP) were detected using a 7890 A GC system (Agilent Technologies) combined with 5975C Inert MS system (Agilent Technologies) as described previously[17]. The total cellular glyceraldehyde 3-phosphate (G3P) concentration was detected according to the protocol of Glycerol-3-Phosphate Assay Kit (ab174094, Abcam)[18].

2.7. ECAR

The ECAR was measured using an XF96 extracellular analyzer (Seahorse Bioscience). A total of 20,000 cells per well were seeded prior to the experiment. The cells were incubated in a CO_2-free incubator at 37 °C, and the medium was changed to XF base medium supplemented with 1 mmol/L pyruvate, 2 mmol/L glutamine, and 10 mmol/L glucose for an hour before measurement. The cells were then sequentially exposed to 2 μmol/L oligomycin and 150 mmol/L 2-deoxyglucose (2-DG). After measurement, the cells were washed with PBS, fixed with 3% PFA, permeabilized with 0.2% triton, and counterstained with Dapi (1:500) to determine the number of cells per well. Data were analyzed using Seahorse XF24 Wave software.

2.8. LS−MS/MS

For the analysis of internal RNA modifications (m^6A, m^5C, and m^1A), polyadenylated RNA was purified from total RNA using two rounds of poly(A) tail purification with the Dynabeads® mRNA DIRECT™ kit (Thermofisher Scientific, #61006). Subsequently, 100 ng of poly(A) RNA was digested with 1 unit of Nuclease P1 (Wako) in a 50 μL buffer containing 10 mmol/L ammonium acetate (pH 5.3) at 42 °C for 5 h. After the addition of 5.5 μL of 1 mol/L fresh NH_4HCO_3 and 1 unit of alkaline phosphatase (Sigma−Aldrich), the mixture was incubated at 37 °C for an additional 5 h. The digested samples were filtered through 0.22-μm syringe filters before being injected into a C18 reverse-phase column coupled online to an Agilent 6460 LC−MS/MS spectrometer in positive electrospray ionization mode for UPLC−MS/MS analysis. Nucleosides were quantified using the nucleoside-to-base ion mass transitions of *m/z* 268.0 to 136.0 (A), *m/z* 282.0 to 150.1 (m^6A), *m/z* 282.0 to 150.0 (m^1A), *m/z* 244.0 to 112.0 (C), *m/z* 258.0 to 126.0 (m^5C), and *m/z* 284.0 to 152.0 (G). Standard curves were generated by running a concentration series of pure commercial nucleosides (Sigma−Aldrich). The concentrations of nucleosides in the samples were calculated by fitting the signal intensities to the standard curves. The m^6A/A, m^1A/A, and m^5C/C ratios were calculated accordingly.

2.9. qRT-PCR

Total RNA was extracted using TRIzol reagent (Invitrogen, Carlsbad, CA, USA) according to the manufacturer's instructions. First-strand cDNA was synthesized using oligo(dT) primers and moloney murine leukemia virus reverse transcriptase (Promega, Madison, WI, USA). Subsequently, 1 μL of the first-strand cDNA synthesis reaction mixture was used for PCR amplification in a total volume of 50 μL. qPCR was performed in triplicate in a 20 μL reaction mixture containing 10 μL of SYBR Premix Ex Taq Master Mix (2 ×) (Takara, Osaka, Japan), 0.5 μmol/L of each primer, and 10 ng cDNA on a Light Cycler® 480 Instrument II (Roche Life Sciences, Meylan, France). The relative expression was calculated using the comparative Ct method. The primer sequences used for amplification are as follows:

GAPDH: Forward: 5′-GTCTCCTCTGACTTCAACAGCG-3′,
Reverse: 5′-ACCACCCTGTTGCTGTAGCCAA-3′;
TRMT6: Forward: 5′-GCAGGAGACATGTCCACTG-3′,
Reverse: 5′-AGGAGAGCTGATCCACTGGA-3′;
TRMT61A: Forward: 5′-GCGCGCAGACAGAACAGAG-3′,
Reverse: 5′-CACAGCCCGTGTAGAAGCAG-3′;
TRMT61B: Forward: 5′-GTCGACGGAACCTGGAGG-3′,
Reverse: 5′-GGGATCAGGGTGGAGGAGG-3′;
TRMT10C: Forward: 5′-ACAGTGATCCCTGCAGCAG-3′,
Reverse: 5′-CCACCTCCACCTGAAATGCT-3′;
NML: Forward: 5′-GGAGACCTGGAGAAGGAGGA-3′,
Reverse: 5′-GAGGCATGGCAGTGTTCTGT-3′;
ALKBH1: Forward: 5′-TGAGCTTGGTGGGAAGTTGA-3′,
Reverse: 5′-TCGTTGTCAGGTAGGCTGGA-3′;
ALKBH3: Forward: 5′-GCTGGAAGATGAGACGCTGA-3′,
Reverse: 5′-TCCTTTGGTCCAGGTTCTGG-3′;

ALKBH7: Forward: 5′-AGACACAGTGGTGACGGGAA-3′;
Reverse: 5′-AGACGTGTGCAGTGACCTTG-3′;
FTO: Forward: 5′-GACGGAGAGGCTTTTGGAGT-3′,
Reverse: 5′-CCCTCAGGATCCATGGAGTA-3′;
ALDOA: Forward: 5′-TTACACAGGCCGCATCTCTC-3′,
Reverse: 5′-GGTTGTGCCTTTCCCTGTAG-3′;
precursor ALDOA Forward: 5′-TCCTTCTTAAAAAAACCAGG-3′,
Reverse: 5′-CTGGGTCGCTAGGGCCCTCC-3′
Firefy-Luc Forward: 5′- GGTACTGTTGGTAAAGCCAC-3′,
Reverse: 5′-CTCTTCATAGCCTTATGCAG-3′
Renilla-Luc Forward: 5′-CAATGGGCAGGTGTCCACTC-3′,
Reverse: 5′-GTTCTGGATCATAAACTTTC-3′.

2.10. Western blot analysis

Cells were lysed with lysis buffer containing RIPA buffer (ThermoFisher Scientific), mini protease inhibitor cocktail complete (Roche), and phosphatase inhibitor (Sigma). Total protein was extracted using TPEB buffer (Invitrogen, Carlsbad, CA, USA). The protein concentration was determined using a BCA analysis kit (Beyotime Biotechnology, Shanghai, China). Typically, 20 μg of protein per lane was resolved by 12% SDS-polyacrylamide gel electrophoresis (PAGE) gels and transferred to a 0.25 μm PVDF membrane (Millipore, Bedford, MA, USA). The membrane was then blocked in TBST containing 5% skimmed milk powder for 1 h and incubated with the following primary antibodies: ALKBH3 (CST, 14916S), ALDOA (Abcam, ab155103), GAPDH (Abcam, ab8245), YTHDF2 (CST, 24744S), PAN2 (CST, 13434S), PAN3 (Abcam, ab214018). The next day, after incubation with HRP-conjugated secondary antibodies (Promega) for 1 h, the membrane was washed with TBST. Finally, the bands were visualized using an enhanced chemiluminescence (ECL) kit (Biosharp, China).

2.11. m^1A-RIP-PCR

Total RNAs were extracted using TRIzol reagent, followed by an additional DNase I treatment to avoid DNA contamination. Then, 40 μg of total RNA was incubated with 1 μg of anti-m^1A antibody in RIP buffer (150 mmol/L NaCl, 0.1% NP-40, 10 mmol/L Tris, pH 7.4) at 4 °C overnight. After incubation, the RNA−antibody complex was added to Protein A/G beads that had been pre-washed with RIP buffer, and the mixture was gently rotated overnight at 4 °C. Beads were washed five times with IPP buffer, and the precipitated RNAs were further purified with TRIzol according to the manufacturer's instructions (Invitrogen, USA). Then, glycogen and isopropanol were added to the supernatant and incubated for 4 h at 4 °C. After washing with 75% ethanol, the pellet was resuspended in RNase-free water for further use. The precipitated RNAs and input RNAs were reverse-transcribed and measured by qPCR. The relative enrichment of m^1A^+ mRNA was calculated as the $2^{-\Delta Ct}$ of m^1A antibody precipitation relative to the input sample[19]. The primer sequences used for amplification of ALDOA are as follows:
5′UTR: Forward: 5′-GCTCCAGAGAATCAGAACAGCC-3′,
Reverser: 5′-CTGCGGCGCTGGCTTCTT-3′;
CDS: Forward: 5′-GGAGTCAAGGGAGGAGGGAG-3′,
Reverse: 5′-ACACGAGACGCCAGGAGG-3′;
3′UTR: Forward: 5′-CGCCTTATAACCAGCCCGGGA-3′,
Reverse: 5′-CGCCGCGCTGCAGCGCG-3′.

2.12. Luciferase assay

Luciferase reporter assays were performed according to the manufacturer's instructions (Promega Inc., CA, USA). The 3′UTR of ALDOA was cloned into the NheI and XbaI sites of the pmirGLO luciferase vector. Cells were transfected with pmirGLO-ALDOA-3′UTR, negative control (NC), and pmirGLO using Lipofectamine 2000 (Invitrogen). After 48 h of culture, the luciferase activity of the cells in different groups was measured using the Dual-Glo Luciferase Assay System (Promega) on a multi-label microplate reader (PerkinElmer EnSpire). The activity of *Renilla* luciferase, used as a control reporter, was used to standardize the luciferase activity. The experiment was repeated 6 times.

2.13. mRNA stability

The mRNA stability of mature and precursor mRNA was measured by treating cells with actinomycin D (Sigma−Aldrich) at a concentration of 2 μg/mL, which inhibits transcription processes induced by RNA polymerase by specifically binding to DNA. RNA transcripts decay and decrease over time after actinomycin D treatment. Total RNA was extracted at 0−4 h and validated by qRT-PCR to check the expression of ALDOA. The RNA degradation curves were plotted, and the mRNA half-life and stability were compared. The mRNA decay rate was determined using a non-linear regression curve fitting (one-phase decay) in GraphPad Prism V9.1 (GraphPad Software, Inc.)

2.14. RIP-PCR

RIP was used to confirm the direct binding of *ALDOA* mRNA with potential binding proteins at the endogenous level using the EZMagna RIP kit (Millipore) according to the manufacturer's protocol *in vitro*. Cells were cross-linked with 1% formaldehyde and lysed with protease and RNase inhibitors. Magnetic beads preincubated with IgG or specific antibodies were incubated with lysates at 4 °C overnight. The protein−RNA complex was then eluted, and qRT-PCR was used to detect the expression of *ALDOA* mRNA. Eluted RNAs were purified and detected with qPCR. Equal quantities of RNA fragments that were not immunoprecipitated were used as the input control.

2.15. Co-immunoprecipitation (Co-IP)

Cells were cultured in a 10-cm dish overnight and lysed with co-IP lysis buffer (Beyotime) at 4 °C for 30 min. After centrifugation at 13,400×*g* for 20 min at 4 °C, 100 μL of the supernatants were aliquoted as "input" samples, and the remaining supernatants were incubated with indicated antibodies overnight at 4 °C under gentle rotation. Protein A + G agarose beads (Beyotime) were added and incubated at 4 °C for an additional 4 h under gentle rotation. The agarose beads were washed five times with IP lysis buffer and boiled with 1 × SDS-PAGE loading buffer. Binding proteins were determined by Western blot analysis.

2.16. Animal study

Female BALB/c nude mice, 8 weeks old, were chosen for xenograft experiments and maintained in specific pathogen-free conditions. All procedures were approved by the First People's Hospital of Foshan Animal Care and Use Committee and followed institutional regulations (C202307-7). The mice were

subcutaneously inoculated with MDA-MB-231 cells (2.5×10^6, 200 μL) stably transfected with sh-control or sh-ALKBH3 vector or infected with lentiviruses (Hanbio Co., Ltd., Shanghai, China) carrying ALDOA ($n = 5$ for each group). Each mouse then received 3 mg/kg of DOX. After 24 days, the mice were sacrificed, and the subcutaneous tumors were excised and weighed. The tumor volume was calculated according to Eq. (1):

$$\text{Tumor volume} = \text{Length} \times \text{Width}^2/2 \quad (1)$$

and measured every three days, and the tumor weight was determined.

2.17. Database analysis

The expression of ALKBH3 and ALDOA in cancers was analyzed using data obtained from the Gene Expression database of Normal and Tumor tissues 2 (GENT2, http://gent2.appex.kr)[20], which integrates publicly available expression profile microarray data from the GEO database to compare and analyze gene expression in normal and cancer patient tissues. The expression profiles of ALKBH3 and ALDOA among the subtypes of breast cancer patients were downloaded from LinkedOmics (http://www.linkedomics.org), which is a publicly available portal that includes multi-omics data from all 32 cancer types from The Cancer Genome Atlas (TCGA) project. To assess the prognostic significance and patient survival, Kaplan−Meier Plots were generated by Kaplan−Meier Plotter (https://kmplot.com/analysis/) with the hazard ratio (HR) and log-rank *P* values calculated on the server's webpage[21].

2.18. Tissue collection and IHC scoring

All patients' samples were sourced from the hospital's biological sample repository. For this analysis, we utilized ten tissue sections from breast cancer patients who exhibited sensitivity to Dox and ten from those who did not. The research proposal underwent thorough review and received approval from the Ethical Committee of The First People's Hospital of Foshan, adhering to the Chinese Ethical Regulations and obtaining written consent from all participants (No. FSYYY-EC-ZN-1.1-A02). Immunohistochemistry (IHC) using ALKBH3 or ALDOA antibody was performed as previously stated[22]. The staining intensity was rated on a scale of 0−3, with 0 representing negative, 1 representing weak, 2 representing medium, and 3 representing strong staining. The staining extent was scored on a scale of 0−4, reflecting the percentage of positive staining areas within the entire tumor area (0% for 0, 1%−25% for 1, 26%−50% for 2, 51%−75% for 3, and 76%−100% for 4). An overall protein expression score (ranging from 0 to 12) was calculated by multiplying the intensity and positivity scores.

2.19. Statistical analysis

Statistical analyses were performed using GraphPad Prism V8.3.0. The data are presented as the mean ± standard deviation (SD). All data represent the mean ± SD of at least three independent experiments. Unpaired two-tailed Student's *t*-test was used to compare differences in cell viability, gene expression, xenograft tumor volume, xenograft tumor weight, and gene expression between different groups. The chi-square test was used to analyze the relationship between gene expression and the clinicopathological features of the patients. Kaplan−Meier curves and log-rank tests were applied to compare the survival of patients with high and low gene expression. In our study, $P < 0.05$ was considered statistically significant.

3. Results

3.1. Dox-resistant TNBC cells exhibited increased glycolysis

We first assessed the Dox sensitivity of both parental and resistance TNBC cells. Our results demonstrated that the induced resistant cells were significantly less sensitive to Dox than their parental cells. The IC_{50} values of Dox for MDA-MB-231/Dox and MDA-MB-231 were 11.9 and 0.85 μmol/L, respectively (Fig. 1A); corresponding values for BT-549/Dox and BT-549 were 13.9 and 1.08 μmol/L (Fig. 1B). These findings confirmed the successful establishment of Dox-resistant TNBC cells.

Chemoresistant cancer cells may show variation in metabolic phenotypes including mitochondrial respiration, oxidative phosphorylation, and aerobic glycolysis[23,24]. Our data showed that both MDA-MB-231/Dox and BT-549/Dox cells exhibited increased ATP generation (Fig. 1C), glucose consumption (Fig. 1D), and lactate production (Fig. 1E) compared to their corresponding parental cells. In addition, Dox-resistant TNBC cells also accumulated higher levels of downstream glycolytic intermediates, including phosphoglycerates (2/3-PGs, Fig. 1F) and phosphoenolpyruvate (PEP, Fig. 1G). Seahorse analysis revealed that the basal and maximal extracellular acidification rate (ECAR) were elevated in Dox-resistant TNBC cells (Fig. 1H and I) compared to their parental cells. This indicated that Dox-resistant TNBC cells showed increased levels of glycolysis and ECAR.

To investigate whether the enhanced glycolysis was involved in Dox resistance of TNBC cells, we further treated cells with glycolysis inhibitors 2-deoxy-D-glucose (2-DG) or oxamate (OX). Our data showed that both 2-DG and OX can significantly restore the Dox sensitivity of MDA-MB-231/Dox (Fig. 1J) and BT-549/Dox (Fig. 1K) cells. Together, these findings indicated that the increased glycolysis contributed to the chemoresistance of TNBC cells.

3.2. ALKBH3-regulated glycolysis in Dox-resistant TNBC cells

Previous studies indicated that epigenetic reprogramming such as RNA modification may act as key regulators of the acquired chemoresistance. We first assessed the m^6A, m^1A and m^5C levels in mRNA from parental and Dox-resistant TNBC cells. Our data showed that both MDA-MB-231/Dox (Fig. 2A) and BT-549/Dox (Fig. 2B) cells exhibited lower m^1A mRNA levels than their parental counterparts. We then focused on the potential roles of m^1A in chemoresistance of TNBC cells.

Since m^1A could be dynamically regulated by methyltransferases called "writer" (TRMT6, TRMT61A, TRMT61B, TRMT10C, and NML) and demethylases called "eraser" (ALKBH1, ALKBH3, ALKBH7, and FTO)[14]. qRT-PCR showed that mRNA levels of *ALKBH3* and *TRMT6* were increased in both MDA-MB-231/Dox (Fig. 2C) and BT-549/Dox (Supporting Information Fig. S1A) cells. Since chemoresistant cells showed decreased m^1A levels, we then checked the expression and potential roles of ALKBH3. Western blot analysis confirmed the upregulation of ALKBH3 in both MDA-MB-231/Dox and BT-549/Dox cells (Fig. 2D).

To investigate whether ALKBH3 was involved in enhancing glycolysis and chemoresistance of TNBC cells, we knocked down its expression in Dox-resistant TNBC cells using shRNA

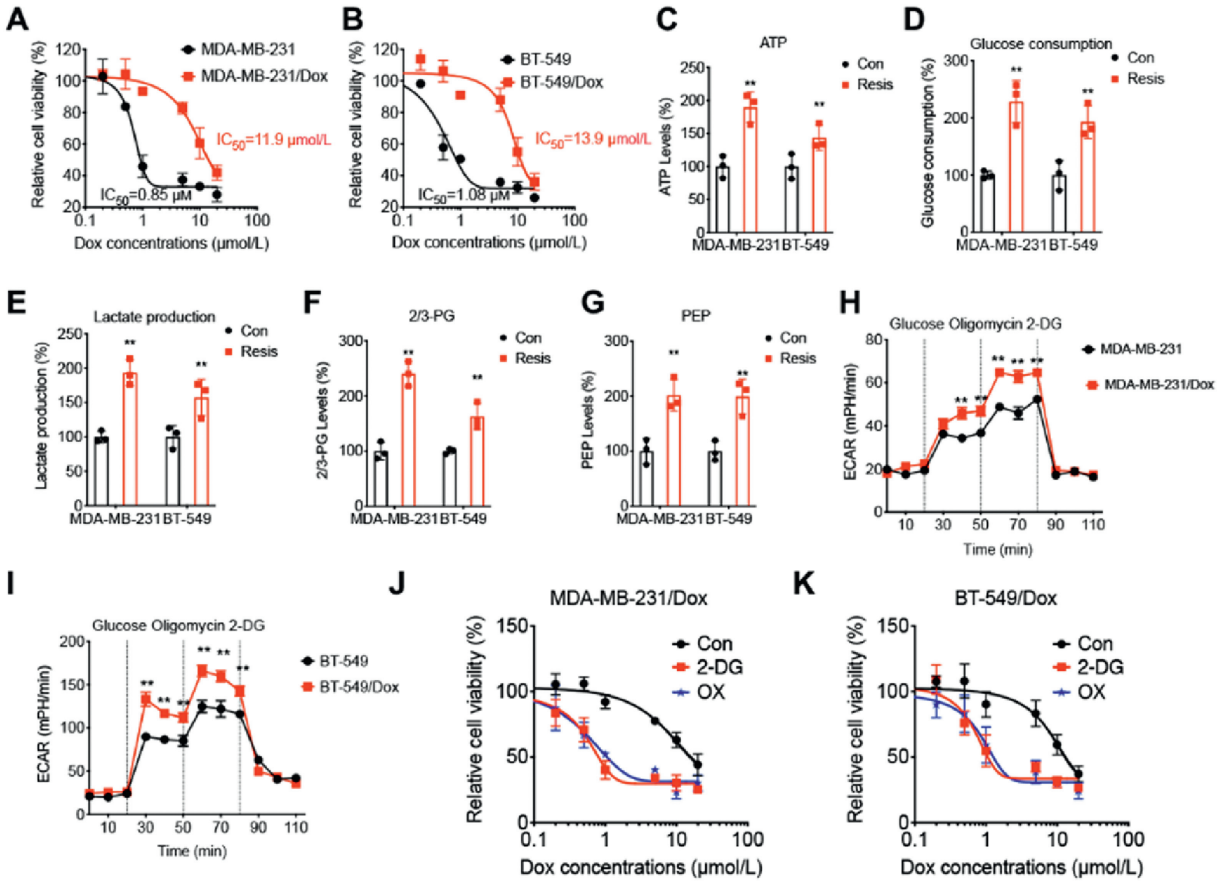

Figure 1 Dox resistant TNBC cells exhibited increased glycolysis. (A, B) Parental or chemoresistant MDA-MB-231 (A) and BT-549 (B) cells were treated with increasing concentration of Dox for 24 h, the cell viability was measured by CCK-8 assay; (C−E) The relative levels of ATP (C), glucose consumption (D), and lactate production (E) of MDA-MB-231/Dox and BT-549/Dox and their parental cells were checked; (F, G) The relative levels of 2/3-FGs (F) and PEP (G) of MDA-MB-231/Dox and BT-549/Dox and their parental cells were checked; (H, I) The extracellular acidification rate (ECAR) levels of MDA-MB-231/Dox (H) and BT-549/Dox (I) and their parental cells were checked; (J, K) MDA-MB-231/Dox (J) and BT-549/Dox (K) cells were pre-treated with or without 2-DG (10 mmol/L) or OX (10 mmol/L) for 90 min and further treated with increasing concentration of Dox for 24 h, the cell viability was measured by CCK-8 assay. Data are presented as mean ± SD. $^{**}P < 0.01$.

(Fig. S1B). Our data showed that sh-*ALKBH3* significantly decreased the ATP generation (Fig. 2E), glucose consumption (Fig. 2F), and lactate production (Fig. 2G) of MDA-MB-231/Dox and BT-549/Dox cells as compared with sh-control cells. Seahorse analysis indicated that the basal and maximal ECAR were decreased in sh-*ALKBH3* MDA-MB-231/Dox (Fig. 2H) and BT-549/Dox (Fig. S1C) cells as compared with that in sh-control cells. In addition, the levels of 2/3-PGs (Fig. S1D) and PEP (Fig. S1E) in sh-*ALKBH3* MDA-MB-231/Dox and BT-549/Dox cells were decreased as compared with those in sh-control cells. Further, the levels of G3P in sh-*ALKBH3* MDA-MB-231/Dox and BT-549/Dox cells were decreased as compared with those in sh-control cells (Fig. S1F). Collectively, these findings demonstrate that ALKBH3 mediates glycolytic reprogramming in Dox-resistant TNBC cells.

3.3. The m^{1}A demethylase activity was essential for ALKBH3-regulated glycolysis of TNBC cells

We further tested whether m^{1}A demethylase activity is essential for ALKBH3-regulated glycolysis and chemosensitivity of TNBC cells. Both MDA-MB-231 and BT-549 cells were transfected with ALKBH3 wild type (WT) or catalytically inactive ALKBH3 mutants (R122S and L177A)[25] (Fig. 3A). LC−MS/MS analysis confirmed that the m1A demethylase activity of ALKBH3 was significantly impaired by the R122S and L177A mutations in both cell lines(Fig. 3B and C).

As to the glycolysis of TNBC cells, our data showed that ALKBH3-WT, but not R122S or L177A, could significantly increase the ATP generation (Fig. 3D), glucose consumption (Fig. 3E), and lactate production (Fig. 3F) of MDA-MB-231 cells. Similarly, ALKBH3-WT, while not R122S or L177A, also increased the ATP generation, glucose consumption, and lactate production of BT-549 cells (Supporting Information Fig. S2A−S2C). Further, overexpression of ALKBH3-WT, while not R122S or L177A, obviously increased the ECAR of both MDA-MB-231 (Fig. 3G) and BT-549 (Fig. S2D) cells. All these data indicated that m^{1}A demethylase activity of ALKBH3 is essential for driving glycolytic reprogramming in TNBC cells.

3.4. ALDOA-mediated ALKBH3-regulated glycolysis of TNBC cells

We next investigated potential targets involved in ALKBH3-regulated glycolysis and chemoresistance of TNBC cells. Since the methylation sites and numbers were varied among different

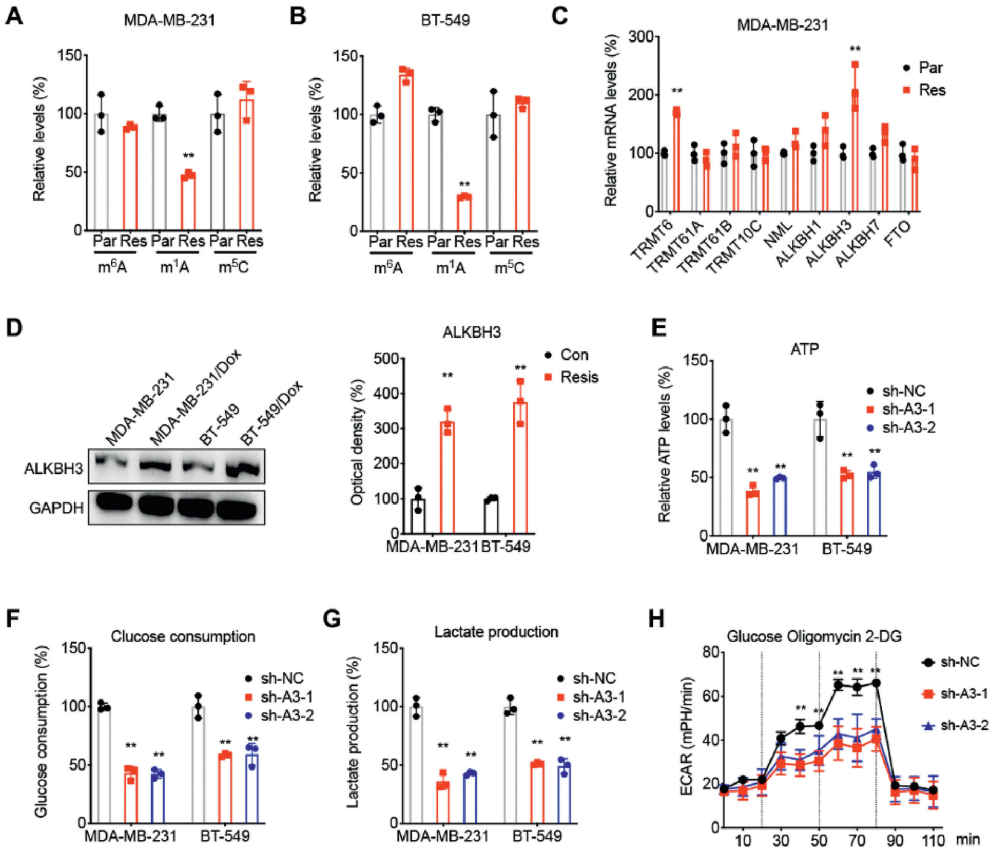

Figure 2 ALKBH3 regulated glycolysis in Dox resistant TNBC cells. (A, B) The relative levels of m^6A, m^1A and m^5C of mRNA collected from MDA-MB-231 (A) and BT-549 (B) and their Dox resistant cells were checked by LC−MS/MS; (C) The relative mRNA levels of m^1A demethylases and methyltransferases in MDA-MB-231/Dox (Res) and MDA-MB-231 (Par) cells were checked by qRT-PCR; (D) The protein levels of ALKBH3 in Dox resistant and parental cells were checked by Western blot analysis (left) and quantitatively analyzed (right); (E−G) The relative levels of ATP (E), glucose consumption (F), and lactate production (G) of sh-control and sh-ALKBH3 MDA-MB-231/Dox and BT-549/Dox cells were checked; (H) The extracellular acidification rate (ECAR) levels of sh-control and sh-ALKBH3 MDA-MB-231/Dox cells. $^{**}P < 0.01$ indicates significance for the sh-NC group compared with sh-A3-1 and sh-A3-2. Data are presented as mean ± SD. $^{**}P < 0.01$.

studies, we analyzed the conserved m^1A modified genes among different studies. There were 1005 conserved m^1A modified genes in HeLa, HEK293T, and HepG2 identified by Dominissini et al.[26] (Supporting Information Fig. S3A), 600 m^1A modified genes in HEK293T identified by Li et al.[19], 2511 m^1A modified genes identified by Esteve-Puig et al.[27], and 1026 genes in m^1A-miCLIP cluster in HEK293T cells identified by Grozhik et al.[28] (Supporting Information Table S1). Among these studies, overlap analysis showed there were 23 conserved m^1A modified genes (Fig. 4A and Table S1). Further, *ALDOA* was the only candidate gene simultaneously observed in four overlap analysis and 200 genes involved in glycolysis (Human Gene Set: HALLMARK_GLYCOLYSIS, Fig. 4B, and Supporting Information Table S2). ALDOA, a key glycolytic enzyme, catalyzes fructose-1,6-bisphosphate (FBP) to G3P and dihydroxyacetone phosphate. It has been implicated in the progression of multiple cancers.[29]. We then investigated whether ALDOA mediates ALKBH3-regulated glycolysis and chemosensitivity of TNBC cells.

Firstly, m^1A RIP-PCR showed that *ALDOA* mRNA was significantly enriched by m^1A antibody in MDA-MB-231 cells, which was diminished in Dox-resistant counterparts (Fig. 4C). Similar results were also observed in BT-549 and BT-549/Dox cells (Fig. S3B). Further, sh-ALKBH3 significantly increased the m^1A enrichment of *ALDOA* mRNA in both MDA-MB-231/Dox (Fig. 4D) and BT-549/Dox (Fig. 4E) cells. In addition, RIP-PCR showed that *ALDOA* mRNA were significantly enriched by ALKBH3 antibody in MDA-MB-231 cells, while this enrichment was increased in MDA-MB-231/Dox cells (Fig. 4F). Similar results were also observed in BT-549/Dox cells (Fig. 4G). Western blot analysis showed that the expression of ALDOA was increased in Dox-resistant breast cancer cells (Fig. 4H). Further, knockdown of ALKBH3 markedly decreased the expression of ALDOA in both MDA-MB-231/Dox and BT-549/Dox cells (Fig. 4I). Further, overexpression of ALKBH3-WT, while not R122S or L177A, can significantly increase the expression of ALDOA in both MDA-MB-231 and BT-549 cells (Fig. 4J). It indicated that ALKBH3 can positively regulate the expression of ALDOA in TNBC cells.

To test whether ALDOA mediates ALKBH3's effects, we rescued ALDOA expression in sh-ALKBH3 cells (Fig. S3C). ALDOA overexpression reversed the suppression of ATP generation, glucose consumption, lactate production caused by ALKBH3 knockdown in MDA-MB-231/Dox cells (Fig. 4K−M). Consistently, overexpression of ALDOA can reverse sh-ALKBH3-suppressed ATP generation, glucose consumption, lactate production in BT-549/Dox cells (Fig. S3D−S3F). Seahorse analysis showed that overexpression of ALDOA can reverse the sh-ALKBH3-suppressed ECAR of MDA-MB-231/Dox (Fig. 4N) and

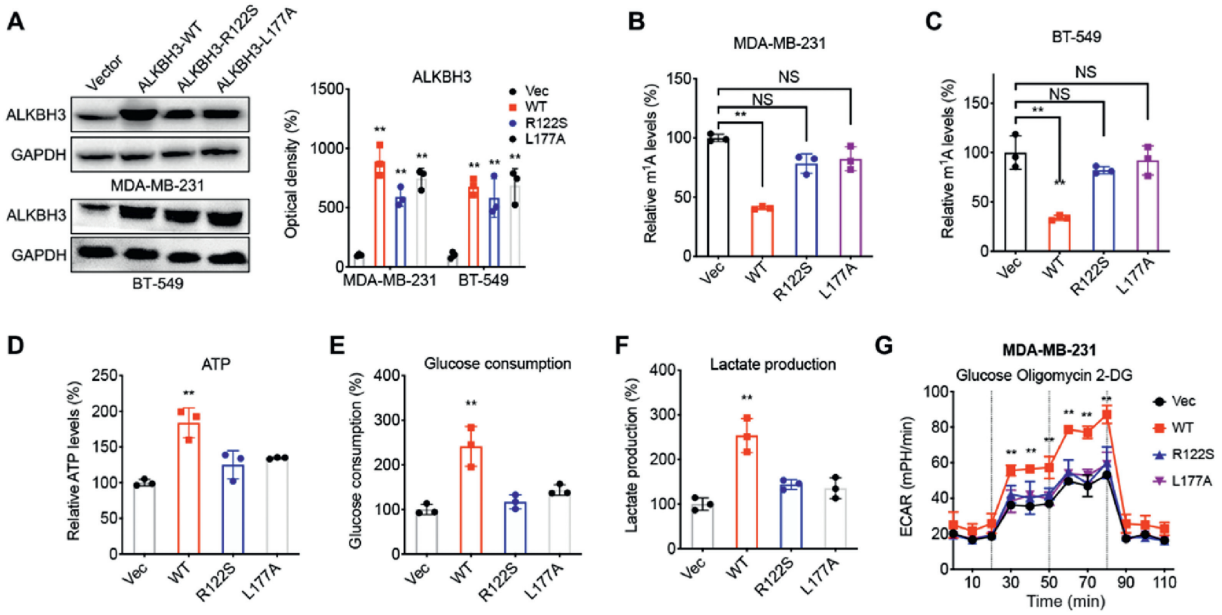

Figure 3 The m^{1}A demethylase activity was essential for ALKBH3-regulated glycolysis of TNBC cells. (A) The protein levels of ALKBH3 in MDA-MB-231 and BT-549 cells transfected with vector control, ALKBH3-WT, R122S or L177A for 24 h; (B, C) The relative m^{1}A levels in mRNA of MDA-MB-231 (B) or BT-549 (C) cells transfected with vector control, ALKBH3-WT, R122S or L177A for 24 h were checked by were checked by LC−MS/MS; (D−F) The relative levels of ATP (D), glucose consumption (E), and lactate production (F) of MDA-MB-231 cells transfected with vector control, ALKBH3-WT, R122S or L177A for 24 h; (G) The extracellular acidification rate (ECAR) levels of MDA-MB-231 cells transfected with vector control, ALKBH3-WT, R122S or L177A for 24 h **$P < 0.01$ indicates significance for the WT group compared with other groups. Data are presented as mean ± SD. **$P < 0.01$; NS, no significant.

BT-549/Dox (Fig. 4O) cells. All these data suggested that ALDOA mediates ALKBH3-regulated glycolysis of TNBC chemoresistant cells.

3.5. *ALKBH3 regulated ALDOA mRNA stability via m^{1}A demethylation at 3′UTR*

We next investigated the mechanisms by which ALKBH3 regulates ALDOA expression in TNBC cells. The results showed that sh-*ALKBH3* significantly decreased the mRNA expression of ALDOA in both MDA-MB-231/Dox and BT-549/Dox cells (Fig. 5A). However, sh-*ALKBH3* had no significant effect on the precursor mRNA of ALDOA in either MDA-MB-231/Dox or BT-549/Dox cells (Fig. 5B). It indicated that *ALKBH3* had no effect on the transcription of ALDOA in TNBC chemoresistant cells. Further, overexpression of ALKBH3-WT, but not the R122S or L177A mutants, significantly increased the mature mRNA expression of ALDOA in both cell lines (Fig. 5C). It indicated that ALKBH3 can positively regulate the mRNA expression of ALDOA in TNBC cells *via* an m^{1}A-dependent manner. Further, our results showed that ALKBH3 knockdown did not affect the translation efficiency of endogenous ALDOA mRNA[30] (Fig. 5D). We therefore focused on the mechanism for ALKBH3/m^{1}A regulated mRNA stability of ALDOA.

Our data showed that sh-ALKBH3 significantly decreased the mRNA stability of *ALDOA* in both MDA-MB-231/Dox (Fig. 5E) and BT-549/Dox (Fig. 5F) cells. In addition, sh-ALKBH3 had no significant effect on the stability of precursor mRNA of *ALDOA* in MDA-MB-231/Dox (Supporting Information Fig. S4A) or BT-549/Dox (Fig. S4B) cells. In addition, overexpression of ALKBH3-WT, while not R122S or L177A, can significantly increase the mRNA stability of *ALDOA* in both MDA-MB-231 (Fig. 5G) and BT-549 (Fig. 5H) cells.

We further investigated the potential m^{1}A methylation site of *ALDOA* in TNBC cells. Fragmented RNA m^{1}A-RIP-PCR revealed that the ALDOA 3′UTR—but not the coding sequence (CDS) or 5′UTR—was enriched in parental MDA-MB-231 cells, with reduced enrichment in Dox-resistant cells (Fig. 5I). Further, sh-*ALKBH3* also increased the m^{1}A enrichment of *ALDOA* 3′UTR in both MDA-MB-231/Dox or BT-549/Dox cells (Fig. 5J). To investigate whether the m^{1}A methylated 3′UTR was involved in ALKBH3-regulated mRNA stability of ALDOA, we subcloned the 3′UTR behind the F-Luc of pmiR-GLO reporter (Fig. 5K). Our data showed that the expression of pmiR-GLO-ALDOA 3′UTR in MDA-MB-231/Dox cells were significantly greater than that of their parental cells (Fig. 5L). Further, sh-ALKBH3 significantly decreased the expression of pmiR-GLO-ALDOA 3′UTR in both MDA-MB-231/Dox and BT-549/Dox cells (Fig. 5M). It was due to that sh-*ALKBH3* can significantly decrease the stability of F-Luc and ALDOA 3′UTR fusion mRNA in both MDA-MB-231/Dox (Fig. 5N) and BT-549/Dox (Fig. 5O) cells. All these data confirmed that ALKBH3 positively regulated *ALDOA* mRNA stability *via* m^{1}A methylation at 3′UTR.

3.6. *m^{1}A negatively regulated mRNA stability of ALDOA via recruitment of YTHDF2/PAN2−PAN3 complex*

We next investigated the potential mechanisms for ALKBH3-regulated mRNA stability of ALDOA. It has been reported that YTHDF1, YTHDF2, YTHDF3, YTHDC1 are m^{1}A-binding proteins called "readers"[25,31-34]. RIP analysis showed that YTHDF2 significantly bound with ALDOA mRNA in both MDA-MB-231

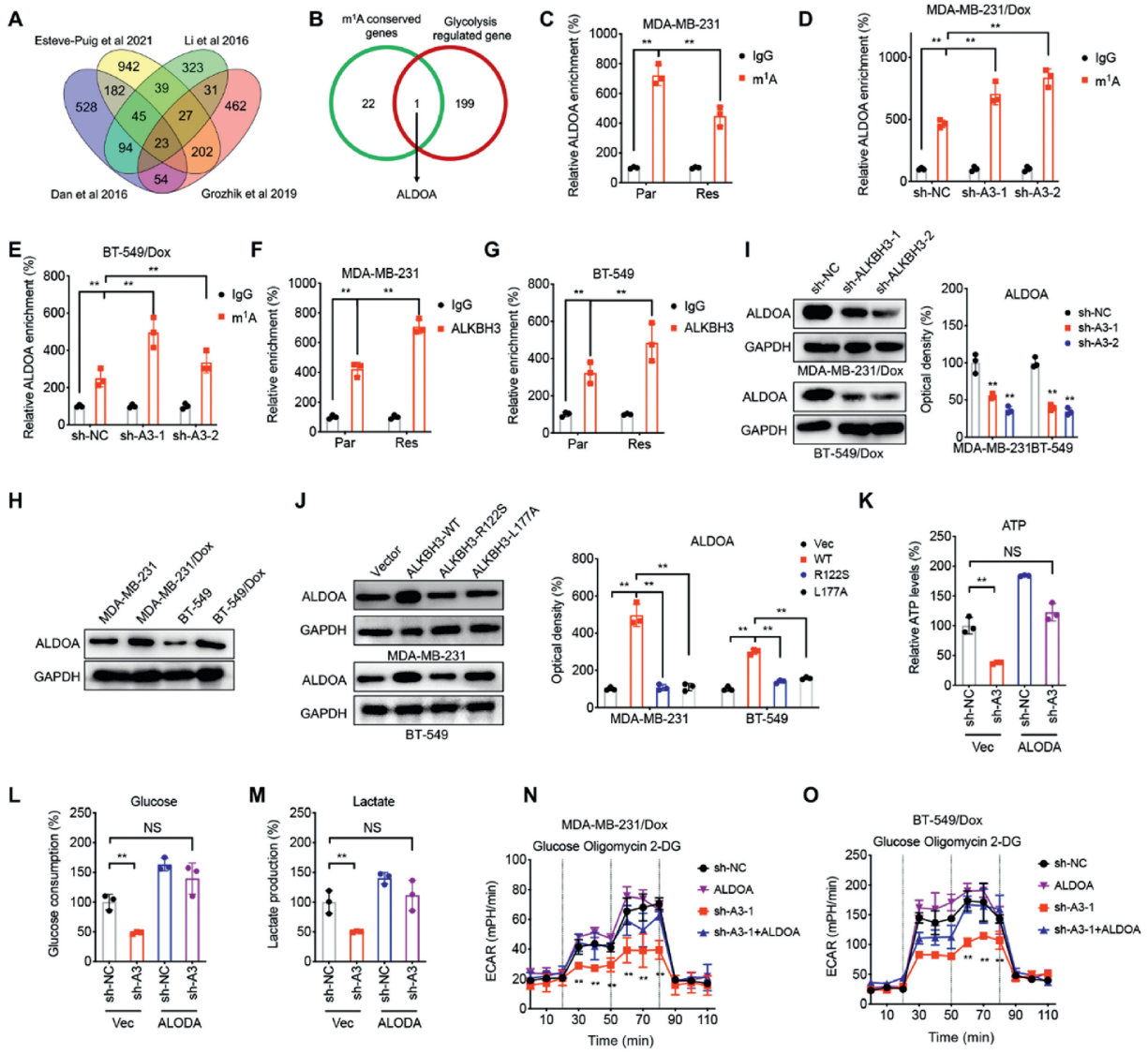

Figure 4 ALDOA mediated ALKBH3-regulated glycolysis of TNBC cells. (A) Venn diagram shows substantial and significant overlap among m^{1}A modified genes HeLa, HEK293T, and HepG2 identified by Dominissini et al.[26], m^{1}A enriched genes in HEK293T identified by Li et al.[19], transcripts containing an m^{1}A-miCLIP cluster in HEK293T cells identified by Grozhik et al.[27], and m^{1}A modified genes identified by Esteve-Puig et al.[28]; (B) Venn diagram shows mRNAs overlap among the glycolysis genes and m^{1}A conserved modified genes in (A); (C) m^{1}A RIP-qPCR analysis of *ALDOA* mRNA m^{1}A enrichment in parental and Dox resistant MDA-MB-231 cells; (D, E) m^{1}A RIP-qPCR analysis of *ALDOA* mRNA m^{1}A enrichment in sh-NC and sh-ALKBH3 MDA-MB-231/Dox (D) and BT-549/Dox (E) cells; (F, G) RIP-qPCR analysis of *ALDOA* mRNA in parental and Dox resistant MDA-MB-231 (F) and BT-549 (G) cells by use of ALKBH3 antibody; (H) The protein expression of ALDOA in parental and Dox resistant MDA-MB-231 and BT-549 cells were checked by Western blot analysis; (I) The protein levels of ALDOA in sh-control and sh-ALKBH3 Dox resistant cells were checked by Western blot analysis (left) and quantitatively analyzed (right); (J) The protein levels of ALDOA in TNBC cells transfected with vector control, ALKBH3-WT, R122S or L177A for 24 h were checked by Western blot analysis (left) and quantitatively analyzed (right); (K−M) The relative levels of ATP (K), glucose consumption (L), and lactate production (M) of sh-control and sh-ALKBH3 MDA-MB-231/Dox cells transfected with vector control or ALDOA for 24 h; (N, O) The extracellular acidification rate (ECAR) levels of sh-control and sh-ALKBH3 MDA-MB-231/Dox (N) or BT-549/Dox (O) cells transfected with vector control or ALDOA for 24 h $^{**}P < 0.01$ indicates significance for the sh-A3-1+ALDOA group compared with other groups. Data are presented as mean ± SD. $^{**}P < 0.01$.

(Fig. 6A) and BT-549 (Fig. 6B) cells. YTHDF2 binding to *ALDOA* mRNA was reduced in TNBC Dox-resistant cells compared to parental cells (Fig. 6C and D). Further, fragmented RNA RIP-PCR showed significant enrichment of *ALDOA* 3′UTR, rather than CDS or 5′UTR, with YTHDF2 in TNBC Dox-resistant cells (Fig. 6E). All these data indicated that YTHDF2 can bind with the m^{1}A methylated 3′UTR of ALDOA.

Further, overexpression of YTHDF2 can significantly decrease the mRNA (Fig. 6F) and protein expression (Fig. 6G) of ALDOA in MDA-MB-231 and BT-549 cells. The sh-control and sh-ALKBH3 MDA-MB-231/Dox cells were further transfected with si-YTHDF2. The results showed that sh-*ALKBH3* induced downregulation of ALDOA was obviously attenuated (Fig. 6H). In addition, overexpression of YTHDF2 can also significantly

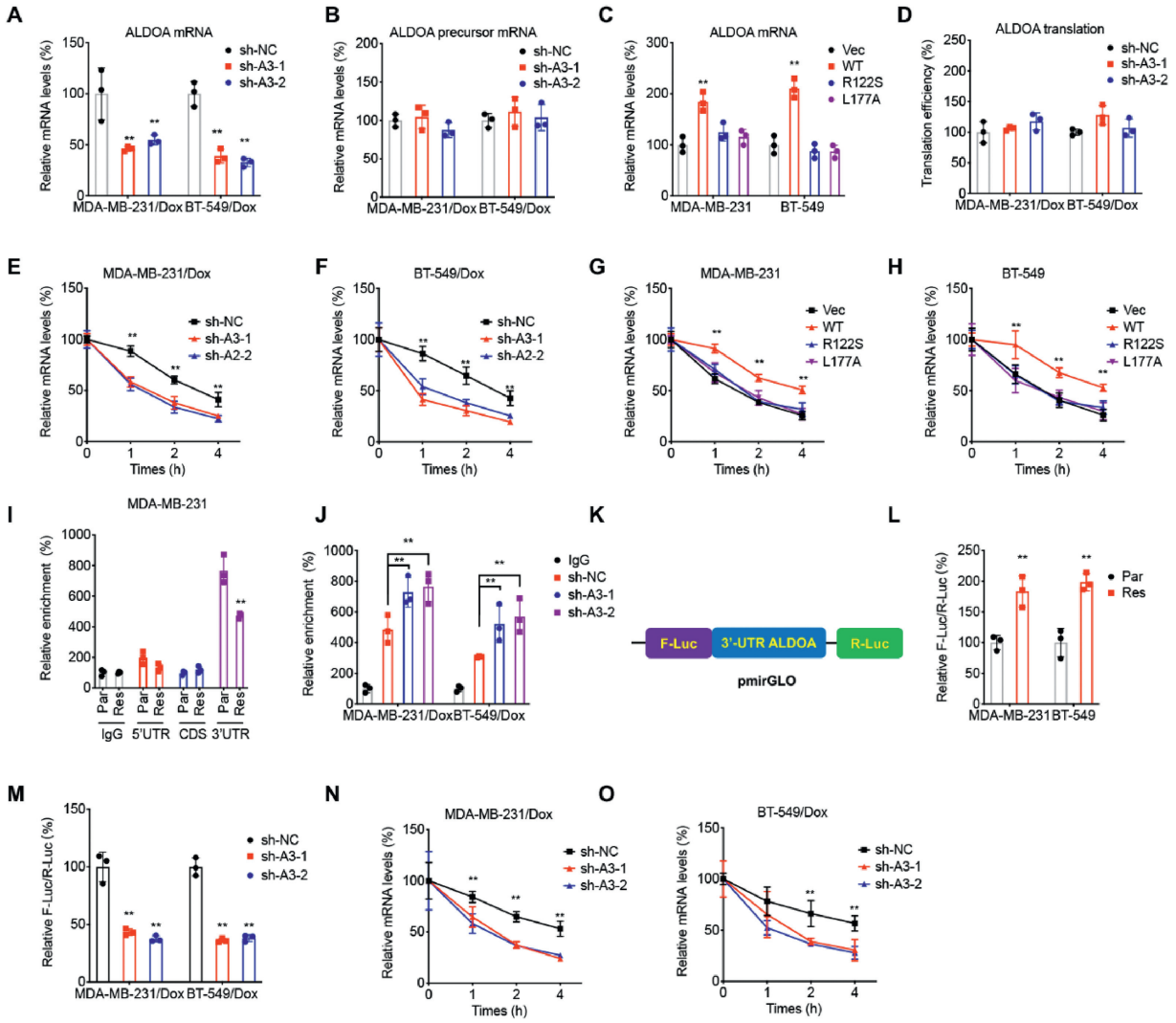

Figure 5 ALKBH3 positively regulated *ALDOA* mRNA stability *via* m^1A methylation at 3′UTR. (A, B) The relative levels of mature (A) or precursor (B) *ALDOA* mRNA in sh-control and sh-ALKBH3 parental and Dox resistant TNBC cells were checked by qRT-PCR; (C) The mRNA levels of *ALDOA* in TNBC cells transfected with vector control, ALKBH3-WT, R122S or L177A for 24 h were checked by qRT-PCR; (D) The translation efficiency of endogenous ALDOA in sh-control and sh-ALKBH3 parental and Dox resistant TNBC cells were checked by normalization of protein levels to the relative mRNA abundance; (E, F) sh-control and sh-ALKBH3 MDA-MB-231/Dox (E) or BT-549/Dox (F) cells were pre-treated with Act-D for 90 min, then mature mRNA of *ALDOA* was analyzed at indicated times, $^{**}P < 0.01$ indicates significance for the sh-NC group compared with other groups; (G, H) MDA-MB-231 (G) and BT-549 (H) cells pre-transfected with vector control, ALKBH3-WT, R122S or L177A for 24 h were further treated with Act-D for 90 min, then mature mRNA of *ALDOA* was analyzed at indicated times, $^{**}P < 0.01$ indicates significance for the WT group compared with other groups; (I) m^1A RIP-qPCR analysis of fragmented *ALDOA* mRNA in parental and Dox resistant MDA-MB-231 cells; (J) m^1A RIP-qPCR analysis of *ALDOA* mRNA 3′UTR in sh-NC or sh-ALKBH3 TNBC Dox resistant cells; (K) Schematic representation of ALDOA 3′UTR of pmirGLO vector to investigate the roles of m^1A in *ALDOA* mRNA stability; (L) The relative F-Luc/R-Luc of pmiR-GLO-ALDOA 3′UTR in parental and Dox resistant TNBC cells; (M) The relative F-Luc/R-Luc of pmiR-GLO-ALDOA 3′UTR in sh-NC or sh-ALKBH3 TNBC Dox resistant cells; (N, O) sh-control and sh-ALKBH3 MDA-MB-231/Dox (N) or BT-549/Dox (O) cells were pre-treated with Act-D for 90 min, then levels of F-Luc-ALDOA 3′UTR fusion RNA was analyzed at indicated times using primers for F-Luc, $^{**}P < 0.01$ indicates significance for the sh-NC group compared with other groups. Data are presented as mean ± SD. $^{**}P < 0.01$.

decrease the expression of pmiR-GLO-ALDOA 3′UTR in MDA-MB-231 and BT-549 cells (Fig. 6I). It was because overexpression of YTHDF2 can significantly decrease the mRNA stability of ALDOA in both MDA-MB-231 and BT-549 cells (Fig. 6J and K). Further, our data showed that the sh-ALKBH3-decreased mRNA stability was attenuated by si-YTHDF2 in MDA-MB-231/Dox cells (Supporting Information Fig. S5A). It indicated that YTHDF2 was responsible for m^1A induced degradation of ALDOA mRNA in cancer cells.

Previous studies indicated that RNA binding proteins can recruit PAN2−PAN3 deadenylase complex to decay target mRNA[35]. Co-IP analysis showed that YTHDF2 can bind with PAN2 and PAN3 in MDA-MB-231/Dox cells (Fig. 6L). Further, RIP-PCR assay showed that both PAN2 (Fig. 6M) and PAN3 (Fig. 6N)

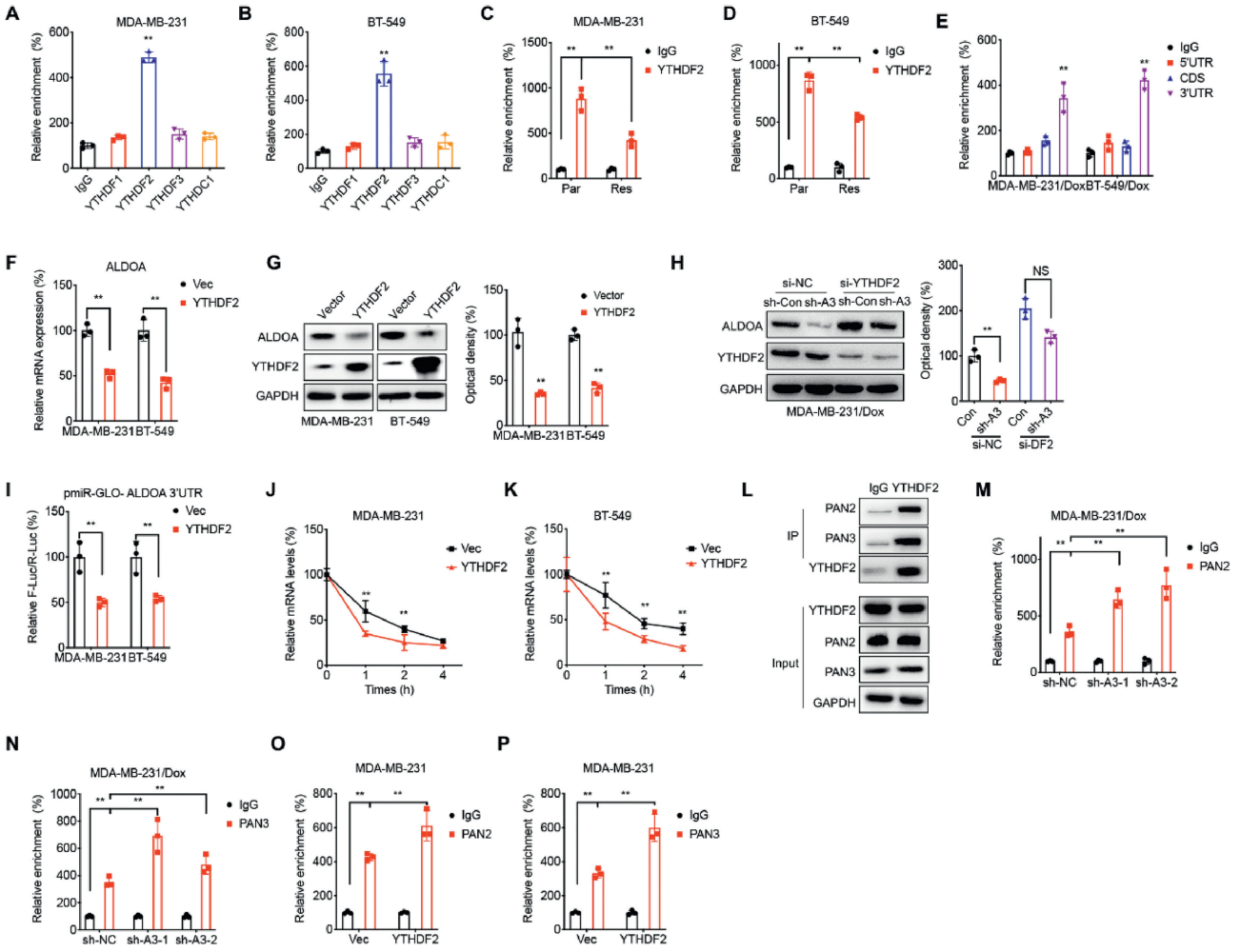

Figure 6 m[1]A negatively regulated mRNA stability of *ALDOA via* recruitment of YTHDF2/PAN2−PAN3 complex. (A, B) The relative binding between *ALDOA* mRNA with potential m[1]A binding proteins YTHDF1/2/3 and YTHDC in MDA-MB-231 (A) and BT-549 (B) cells; (C, D) The relative enrichment of *ALDOA* mRNA levels with YTHDF2 in parental and Dox resistant MDA-MB-231 (C) and BT-549 (D) cells; (E) RIP-qPCR analysis of fragmented *ALDOA* mRNA in Dox resistant TNBC cells by use of anti-YTHDF2; (F, G) Cells were transfected with vector control or YTHDF2 constructs for 24 h, the mRNA (F) and protein (G) levels of ALDOA were checked; (H) The sh-Control and sh-ALKBH3 MDA-MB-231/Dox cells were further transfected with si-YTHDF2 for 24 h, the protein expression of ALDOA was checked; (I) The relative F-Luc/R-Luc of pmiR-GLO-ALDOA 3′UTR in cells pre-transfected with vector control or YTHDF2 constructs for 24 h; (J, K) MDA-MB-231 (J) or BT-549 (K) cells pre-transfected with vector control or YTHDF2 constructs for 24 h were further treated with Act-D for 90 min, then precursor mRNA of *ALDOA* was analyzed at indicated times; (L) Binding between YTHDF2 with PAN2 or PAN3 were checked by immunoprecipitation by pull-down of YTHDF2 in MDA-MB-231/Dox cells; (M, N) The RIP-qPCR analysis of *ALDOA* mRNA in sh-control and sh-ALKBH3 MDA-MB-231/Dox cells by use of anti-PAN2 (M) or PAN3 (N); (O, P) The RIP-qPCR analysis of *ALDOA* mRNA by use of anti-PAN2 (O) or PAN3 (P) in MDA-MB-231 cells pre-transfected with vector control or YTHDF2 constructs for 24 h. Data are presented as mean ± SD. $^{**}P < 0.01$.

can directly bind with mRNA of ALDOA in MDA-MB-231/Dox cells, while the binding was increased in sh-*ALKBH3* knockdown cells. In addition, RIP-PCR assay showed that both sh-*ALKBH3* can increase the binding between mRNA of ALDOA with PAN2 and PAN3 in BT-549/Dox cells (Fig. S5B and S5C). We further investigate whether YTHDF2 was essential for PAN2−PAN3 induced degradation of ALDOA. The results showed that overexpression of YTHDF2 can significantly increase the binding between PAN2 and ALDOA mRNA (Fig. 6O) and binding between *PAN3* and *ALDOA* mRNA (Fig. 6P) in MDA-MB-231 cells. The data suggested that YTHDF2 can recruit PAN2−PAN3 to induce the decay of m[1]A methylated ALDOA mRNA in TNBC chemoresistant cells.

3.7. ALKBH3/ALDOA axis promoted the in vitro and in vivo Dox resistance

We further checked the effect of ALKBH3/ALDOA on Dox sensitivity of TNBC cells. ALKBH3 knockdown resensitized both MDA-MB-231/Dox (Fig. 7A) and BT-549/Dox (Fig. 7B) to Dox treatment. Our data showed that overexpression of ALKBH3-WT, while not R122S or L177A, can significantly decrease the Dox sensitivity of MDA-MB-231 cells (Fig. 7C). Consistently, ALKBH3-WT, while not R122S or L177A, can also significantly decrease the Dox sensitivity of BT-549 cells (Fig. 7D). These data demonstrate that ALKBH3 promotes chemoresistance in TNBC cells through its m[1]A demethylase activity.

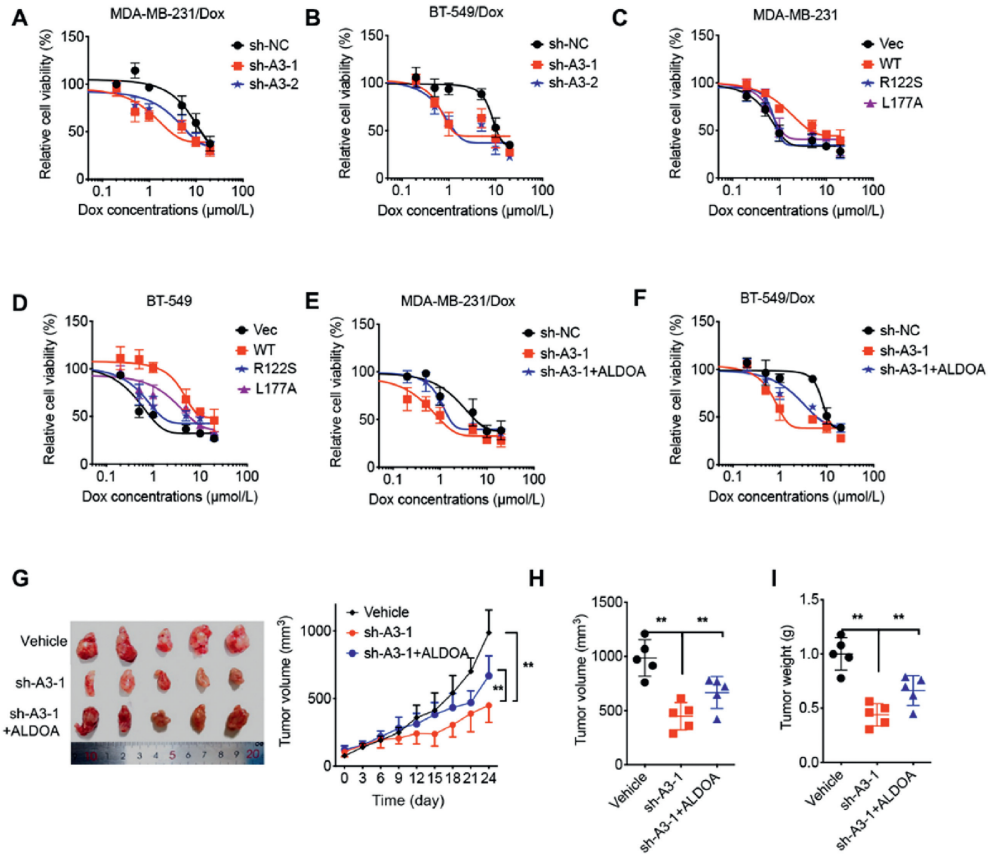

Figure 7 ALKBH3/ALDOA axis promotes the *in vitro* and *in vivo* Dox resistance. (A, B) The sh-control and sh-ALKBH3 MDA-MB-231/Dox (A) and BT-549/Dox (B) cells were treated with increasing concentration of Dox for 24 h; (C, D) MDA-MB-231 (C) or BT-549 (D) cells pre-transfected with vector control, ALKBH3-WT, R122S or L177A for 24 h and further treated with increasing concentration of Dox for 24 h; (E, F) The sh-control and sh-ALKBH3 MDA-MB-231/Dox (E) and BT-549/Dox (F) cells with or without ALDOA constructs for 24 h and then further were treated with increasing concentration of Dox for 24 h; (G—I) Xenografts of sh-control and sh-ALKBH3 MDA-MB-231/Dox cells with or without ALDOA constructs were treated with Dox. (G) The tumor growth curves were recorded every three days; tumor volume (H) and weight (I) of xenografts for each group at the end of experiments. Data are presented as mean ± SD. $^{**}P < 0.01$.

We further checked whether ALDOA was involved in ALKBH3-regulated Dox sensitivity. Our data showed that overexpression of ALDOA can reverse sh-ALKBH3 increased Dox sensitivity of both MDA-MB-231/Dox (Fig. 7E) and BT-549/Dox cells (Fig. 7F). This result suggested that ALKBH3/ALDOA axis regulated Dox resistance of TNBC cells. To verify the *in vivo* effects, mice were implanted with sh-control, sh-ALKBH3, sh-ALKBH3+ALDOA MDA-MB-231/Dox cells and then further treated with Dox. Our data showed that sh-ALKBH3 can increase the *in vivo* Dox sensitivity, while overexpression of ALDOA can reverse sh-ALKBH3 increased Dox sensitivity (Fig. 7G). Further, tumor volume and weight in sh-ALKBH3+ALDOA were significantly greater than those in sh-ALKBH3 group (Fig. 7H and I). IHC analysis showed that the expression of ALDOA was decreased after knockdown of ALKBH3 in the xenografts (Supporting Information Fig. S6). This result suggested that ALKBH3/ALDOA axis regulated Dox resistance of TNBC cells.

3.8. Clinical characteristics of ALKBH3/ALDOA axis on TNBC progression

We further evaluated the clinical relevance of ALKBH3/ALDOA axis on TNBC progression. Data from GNET2 indicated that the expression of *ALKBH3* (Fig. 8A) and *ALDOA* (Fig. 8B) in breast cancer tissues was significantly ($P < 0.01$) higher than those in normal tissues[20]. In addition, the expression levels of ALKBH3 in ER^- (Fig. 8C), $HER2^-$ (Fig. 8D), and PR^- (Fig. 8E) breast cancer tissues were significantly greater than those in ER^+, HER^+, and PR^+ breast cancer tissues. Similarly, the xpression levels of ALDOA in ER^- (Fig. 8F), $HER2^-$ (Fig. 8G), and PR^- (Fig. 8H) breast cancer tissues were significantly greater than those in ER^+, HER^+, and PR^+ breast cancer tissues. Further, ALDOA expression positively correlated with ALKBH3 (Fig. 8I) but inversely correlated with YTHDF2 (Fig. 8J), PAN2 (Fig. 8K), and PAN3 (Fig. 8L) in breast cancer patients. Using the online bioinformatics tool Kaplan—Meier plotter[21], we found that TNBC patients with high expression of ALKBH3 (Fig. 8M) and ALDOA (Fig. 8N) had significantly reduced overall survival (OS) than those with their corresponding low expression patients.

Furthermore, we collected tissues from breast cancer patients, stratified into drug-sensitive ($n = 10$) and drug-resistant ($n = 10$) cohorts, to assess the expression levels of ALKBH3 and ALDOA. The IHC results demonstrated a significant increase in the expression of both ALKBH3 and ALDOA in tissues derived from drug-resistant patients compared to those from sensitive patients (Fig. 8O). The results indicated that ALKBH3/ALDOA axis drives oncogenic progression in the clinical progression of TNBC patients.

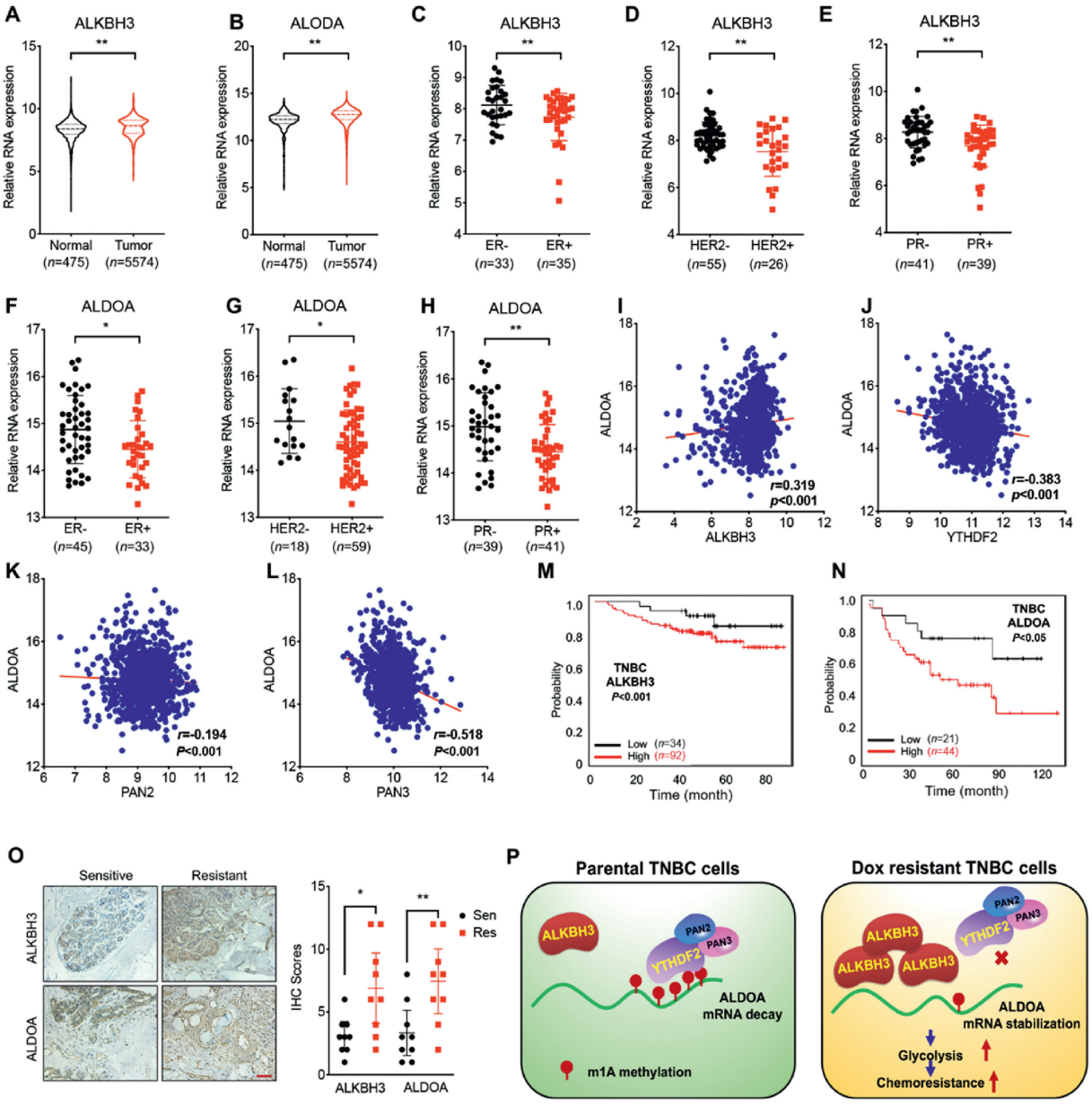

Figure 8 Clinical characteristics of ALKBH3/ALDOA axis on TNBC progression. (A, B) The expression of ALKBH3 (A) and ALDOA (B) in breast cancer and normal tissues with the data from GNET2[29]; (C−E) The expression of ALKBH3 in ER (C), HER2 (D), and PR (E) positive or negative breast cancer tissues; (F−H) The expression of ALDOA in ER (F), HER2 (G), and PR (H) positive or negative breast cancer tissues; (I−L) Correlation between *ALDOA* and ALKBH3 (I), YTHDF2 (J), PAN2 (K), and PAN3 (L) in breast cancer patients from TCGA database; (M, N) The Kaplan−Meier survival curves of OS based on ALKBH3 (M) and ALDOA (N) expression in breast cancer patients from TCGA data base; (O) IHC (ALKBH3 and ALDOA)-stained paraffin-embedded sections obtained from tumor tissues of sensitive and drug resistant breast cancer patients. The scale bar is 100 μm. (P) Proposed model to illustrate the mechanisms of m^1A-regulated mRNA stability of *ALDOA* in Dox resistant TNBC cells. $^*P < 0.05$, $^{**}P < 0.01$.

4. Discussion

Due to the lack of corresponding therapeutic targets, TNBC cannot benefit from endocrine therapy or targeted therapy; thus, chemotherapy is currently the primary systemic treatment for TNBC. Adriamycin, a cytotoxic drug inhibiting RNA and DNA synthesis, is widely used in the treatment of TNBC due to its high efficacy. Unfortunately, the development of chemoresistance remains a major hurdle to its use and limits its effectiveness[36]. Therefore, elucidating the mechanisms underlying TNBC chemoresistance is critical. Our data indicated that Dox-resistant TNBC cells showed enhanced glycolysis. Moreover, glycolysis inhibition restored Dox sensitivity. This was consistent with recent studies that chemoresistant cells can reprogram metabolic profiles such as glycolysis and glutamine metabolism to suppress chemotherapy efficiency[37] and targeting glycolysis might be a novel strategy to overcome drug resistance in cancer cells[38,39].

Our data revealed that targeting glycolysis might be a potential therapeutic target to overcome Dox resistance of TNBC cells.

Our data showed that ALKBH3 regulates the glycolysis and chemoresistance of TNBC cells *via* m^1A demethylase activity. The biological functions and roles of m^1A in cancer remain poorly understood. ALKBH3 has been found to promote the proliferation of cancer cells from gastrointestinal cancer[40,41], hepatocellular carcinoma[42], glioma[43], prostate cancer[44,45], and colorectal cancer[46]. Further, ALKBH3 can also promote cancer cell invasion *via* destabilizing tRNAs[25]. Recently, ALKBH3 promotes the glycolysis of cancer cells by modulating the expression of m^1A-modified *ATP5D* mRNA[16]. Our data showed that ALKBH3 was increased in TNBC chemoresistant cells, while knockdown of ALKBH3 can re-sensitize cells to Dox treatment. Further, overexpression of wild-type ALKBH3, while not m^1A catalytically inactive ALKBH3 mutants, can decrease Dox sensitivity of TNBC cells. To our knowledge, this is the first study to link ALKBH3 and m^1A mRNA methylation to cancer drug resistance.

Our data indicated that ALDOA mediates ALKBH3-regulated glycolysis and Dox resistance of TNBC cells. Mechanistically, we found that the increased ALKBH3 in Dox-resistant cells can demethylate m^1A at 3′UTR of *ALDOA* mRNA, resulting in the decreased binding with reader protein YTHDF2, which finally leads to the upregulation of *ALDOA* mRNA stability and enhancing glycolysis in resistant cells. It has been revealed that m^1A is associated with the mRNA destabilization mediated by reader proteins YTHDF2 and YTHDF3[47-49]. Our present study further revealed that the m^1A reader protein YTHDF2 can recruit PAN2−PAN3 complex to decay *ALDOA* mRNA in TNBC cells, while the upregulation of ALKBH3 in Dox-resistant cells suppresses this degradation. Recent study also indicated that m^1A of *ATP5D* mRNA can recruit m^1A reader YTHDF1, which forms a complex with eRF1, to facilitate translation termination and decrease translation efficiency[16]. It indicated that important roles and diversity functions of m^1A in mRNA.

Collectively, our data present study indicated that ALKBH3 upregulation reduces m^1A methylation on *ALDOA* mRNA, enhancing its stability and glycolytic activity in Dox-resistant TNBC cells (Fig. 8P). Mechanistically, ALKBH3 can demethylate the 3′UTR of *ALDOA* mRNA to increase its mRNA stability *via* impairing the binding with YTHDF2 and recruiting PAN2−PAN3 complex. Our study provided that ALKBH3/ALDOA axis-induced glycolysis should be a potential therapy target to overcome Dox resistance in TNBC cells.

Acknowledgements

This study was funded by the Research Project of TCM Bureau of Guangdong Province (20231324, China), the Special Fund of Foshan Climbing Peak Plan (2020B018, China), the Basic and Applied Basic Research Foundation of Guangdong Province (Grant No. 2022A1515140091, China), and the Natural Science Foundation of Guangdong Province (2023A1515030291, China).

Author contributions

Yuhua Deng: Investigation, Data curation, Conceptualization. Zhiyan Chen: Methodology, Investigation. Peixian Chen: Methodology, Investigation. Yaming Xiong: Resources, Methodology. Chuling Zhang: Project administration. Qiuyuan Wu: Resources, Investigation. Huiqi Huang: Formal analysis, Data curation. Shuqing Yang: Validation. Kun Zhang: Validation, Investigation. Tiancheng He: Methodology, Investigation. Wei Li: Resources, Methodology. Guolin Ye: Methodology. Wei Luo: Validation, Supervision. Hongsheng Wang: Validation, Supervision. Dan Zhou: Writing − review & editing, Writing − original draft, Visualization, Funding acquisition.

Conflicts of interest

The authors declare no conflict of interest.

Appendix A. Supporting information

Supporting information to this article can be found online at https://doi.org/10.1016/j.apsb.2025.04.018.

References

1. Treeck O, Schuler-Toprak S, Ortmann O. Estrogen actions in triple-negative breast cancer. *Cells* 2020;**9**:2358.
2. Pasha N, Turner NC. Understanding and overcoming tumor heterogeneity in metastatic breast cancer treatment. *Nat Can (Ott)* 2021;**2**:680−92.
3. Nederlof I, Voorwerk L, Kok M. Facts and hopes in immunotherapy for early-stage triple-negative breast cancer. *Clin Cancer Res* 2023;**29**: 2362−70.
4. Bai X, Ni J, Beretov J, Graham P, Li Y. Triple-negative breast cancer therapeutic resistance: where is the Achilles' heel?. *Cancer Lett* 2021; **497**:100−11.
5. Derouane F, Desgres M, Moroni C, Ambroise J, Berliere M, Van Bockstal MR, et al. Metabolic adaptation towards glycolysis supports resistance to neoadjuvant chemotherapy in early triple negative breast cancers. *Breast Cancer Res* 2024;**26**:29.
6. Zhou M, Zhao Y, Ding Y, Liu H, Liu Z, Fodstad O, et al. Warburg effect in chemosensitivity: targeting lactate dehydrogenase-A re-sensitizes taxol-resistant cancer cells to taxol. *Mol Cancer* 2010;**9**:33.
7. Kawai K, Uemura M, Munakata K, Takahashi H, Haraguchi N, Nishimura J, et al. Fructose-bisphosphate aldolase A is a key regulator of hypoxic adaptation in colorectal cancer cells and involved in treatment resistance and poor prognosis. *Int J Oncol* 2017;**50**:525−34.
8. Varghese E, Samuel SM, Liskova A, Samec M, Kubatka P, Busselberg D. Targeting glucose metabolism to overcome resistance to anticancer chemotherapy in breast cancer. *Cancers (Basel)* 2020;**12**:2252.
9. Ponnusamy L, Mahalingaiah PKS, Singh KP. Epigenetic reprogramming and potential application of epigenetic-modifying drugs in acquired chemotherapeutic resistance. *Adv Clin Chem* 2020;**94**:219−59.
10. Berdasco M, Esteller M. Towards a druggable epitranscriptome: compounds that target RNA modifications in cancer. *Br J Pharmacol* 2022;**179**:2868−89.
11. Liu Z, Zou H, Dang Q, Xu H, Liu L, Zhang Y, et al. Biological and pharmacological roles of m^6A modifications in cancer drug resistance. *Mol Cancer* 2022;**21**:220.
12. Shi Y, Dou Y, Zhang J, Qi J, Xin Z, Zhang M, et al. The RNA N^6-methyladenosine methyltransferase METTL3 promotes the progression of kidney cancer *via* N^6-methyladenosine-dependent translational enhancement of ABCD1. *Front Cell Dev Biol* 2021;**9**:737498.
13. Zheng Q, Yu X, Zhang Q, He Y, Guo W. Genetic characteristics and prognostic implications of m^1A regulators in pancreatic cancer. *Biosci Rep* 2021;**41**:BSR20210337.
14. Li J, Zhang H, Wang H. N^1-Methyladenosine modification in cancer biology: current status and future perspectives. *Comput Struct Biotechnol J* 2022;**20**:6578−85.
15. Chen Y, Zhang K, Li Y, Guo R, Zhang K, Zhong G, et al. Oestrogen-related receptor alpha mediates chemotherapy resistance of osteosarcoma cells *via* regulation of ABCB1. *J Cell Mol Med* 2019;**23**: 2115−24.

16. Wu YM, Chen ZJ, Xie GY, Zhang HS, Wang ZT, Zhou JW, et al. RNA m^1A methylation regulates glycolysis of cancer cells through modulating ATP5D. *Proc Natl Acad Sci U S A* 2022;**119**:e2119038119.
17. Rossi M, Altea-Manzano P, Demicco M, Doglioni G, Bornes L, Fukano M, et al. PHGDH heterogeneity potentiates cancer cell dissemination and metastasis. *Nature* 2022;**605**:747−53.
18. Xie J, Ye J, Cai Z, Luo Y, Zhu X, Deng Y, et al. GPD1 enhances the anticancer effects of metformin by synergistically increasing total cellular glycerol-3-phosphate. *Cancer Res* 2020;**80**:2150−62.
19. Li X, Xiong X, Wang K, Wang L, Shu X, Ma S, et al. Transcriptome-wide mapping reveals reversible and dynamic N^1-methyladenosine methylome. *Nat Chem Biol* 2016;**12**:311−6.
20. Park SJ, Yoon BH, Kim SK, Kim SY. GENT2: an updated gene expression database for normal and tumor tissues. *BMC Med Genom* 2019;**12**:101.
21. Lanczky A, Gyorffy B. Web-based survival analysis tool tailored for medical research (KMplot): development and implementation. *J Med Internet Res* 2021;**23**:e27633.
22. Zhou Y, Lu L, Jiang G, Chen Z, Li J, An P, et al. Targeting CDK7 increases the stability of Snail to promote the dissemination of colorectal cancer. *Cell Death Differ* 2019;**26**:1442−52.
23. Lukey MJ, Katt WP, Cerione RA. Targeting therapy resistance: when glutamine catabolism becomes essential. *Cancer Cell* 2018;**33**:795−7.
24. Wicki A, Mandala M, Massi D, Taverna D, Tang HF, Hemmings BA, et al. Acquired resistance to clinical cancer therapy: a twist in physiological signaling. *Physiol Rev* 2016;**96**:805−29.
25. Chen Z, Qi M, Shen B, Luo G, Wu Y, Li J, et al. Transfer RNA demethylase ALKBH3 promotes cancer progression *via* induction of tRNA-derived small RNAs. *Nucleic Acids Res* 2019;**47**:2533−45.
26. Dominissini D, Nachtergaele S, Moshitch-Moshkovitz S, Peer E, Kol N, Ben-Haim MS, et al. The dynamic N^1-methyladenosine methylome in eukaryotic messenger RNA. *Nature* 2016;**530**:441−6.
27. Esteve-Puig R, Climent F, Pineyro D, Domingo-Domenech E, Davalos V, Encuentra M, et al. Epigenetic loss of m^1A RNA demethylase ALKBH3 in Hodgkin lymphoma targets collagen, conferring poor clinical outcome. *Blood* 2021;**137**:994−9.
28. Grozhik AV, Olarerin-George AO, Sindelar M, Li X, Gross SS, Jaffrey SR. Antibody cross-reactivity accounts for widespread appearance of m^1A in 5′UTRs. *Nat Commun* 2019;**10**:5126.
29. Li D, Wang X, Li G, Dang Y, Zhao S, Qin Y. LncRNA ZNF674-AS1 regulates granulosa cell glycolysis and proliferation by interacting with ALDOA. *Cell Death Discov* 2021;**7**:107.
30. Wang X, Zhao BS, Roundtree IA, Lu Z, Han D, Ma H, et al. N^6-Methyladenosine modulates messenger RNA translation efficiency. *Cell* 2015;**161**:1388−99.
31. Chujo T, Suzuki T. Trmt61B is a methyltransferase responsible for 1-methyladenosine at position 58 of human mitochondrial tRNAs. *RNA* 2012;**18**:2269−76.
32. Safra M, Sas-Chen A, Nir R, Winkler R, Nachshon A, Bar-Yaacov D, et al. The m^1A landscape on cytosolic and mitochondrial mRNA at single-base resolution. *Nature* 2017;**551**:251−5.
33. Dai X, Wang T, Gonzalez G, Wang Y. Identification of YTH domain-containing proteins as the readers for N^1-methyladenosine in RNA. *Anal Chem* 2018;**90**:6380−4.
34. Waku T, Nakajima Y, Yokoyama W, Nomura N, Kako K, Kobayashi A, et al. NML-mediated rRNA base methylation links ribosomal subunit formation to cell proliferation in a p53-dependent manner. *J Cell Sci* 2016;**129**:2382−93.
35. Liu JD, Gao MW, Xu SY, Chen YP, Wu KX, Liu H, et al. YTHDF2/3 are required for somatic reprogramming through different RNA deadenylation pathways. *Cell Rep* 2020;**32**:108120.
36. Nedeljkovic M, Damjanovic A. Mechanisms of chemotherapy resistance in triple-negative breast cancer-how we can rise to the challenge. *Cells* 2019;**8**:957.
37. Belisario DC, Kopecka J, Pasino M, Akman M, De Smaele E, Donadelli M, et al. Hypoxia dictates metabolic rewiring of tumors: implications for chemoresistance. *Cells* 2020;**9**:2598.
38. Cheng C, Xie Z, Li Y, Wang J, Qin C, Zhang Y. PTBP1 knockdown overcomes the resistance to vincristine and oxaliplatin in drug-resistant colon cancer cells through regulation of glycolysis. *Biomed Pharmacother* 2018;**108**:194−200.
39. Xu RH, Pelicano H, Zhou Y, Carew JS, Feng L, Bhalla KN, et al. Inhibition of glycolysis in cancer cells: a novel strategy to overcome drug resistance associated with mitochondrial respiratory defect and hypoxia. *Cancer Res* 2005;**65**:613−21.
40. Li J, Zuo Z, Lai S, Zheng Z, Liu B, Wei Y, et al. Differential analysis of RNA methylation regulators in gastric cancer based on TCGA data set and construction of a prognostic model. *J Gastrointest Oncol* 2021;**12**:1384−97.
41. Zhao Y, Zhao Q, Kaboli PJ, Shen J, Li M, Wu X, et al. m^1A regulated genes modulate PI3K/AKT/mTOR and ErbB pathways in gastrointestinal cancer. *Transl Oncol* 2019;**12**:1323−33.
42. Shi Q, Xue C, Yuan X, He Y, Yu Z. Gene signatures and prognostic values of m^1A-related regulatory genes in hepatocellular carcinoma. *Sci Rep* 2020;**10**:15083.
43. Macari F, El-Houfi Y, Boldina G, Xu H, Khoury-Hanna S, Ollier J, et al. TRM6/61 connects PKCalpha with translational control through tRNAi(Met) stabilization: impact on tumorigenesis. *Oncogene* 2016;**35**:1785−96.
44. Konishi N, Nakamura M, Ishida E, Shimada K, Mitsui E, Yoshikawa R, et al. High expression of a new marker PCA-1 in human prostate carcinoma. *Clin Cancer Res* 2005;**11**:5090−7.
45. Ueda Y, Ooshio I, Fusamae Y, Kitae K, Kawaguchi M, Jingushi K, et al. AlkB homolog 3-mediated tRNA demethylation promotes protein synthesis in cancer cells. *Sci Rep* 2017;**7**:42271.
46. Gao Y, Wang H, Li H, Ye X, Xia Y, Yuan S, et al. Integrated analyses of m^1A regulator-mediated modification patterns in tumor microenvironment-infiltrating immune cells in colon cancer. *OncoImmunology* 2021;**10**:1936758.
47. Seo KW, Kleiner RE. YTHDF2 recognition of N^1-methyladenosine (m^1A)-modified RNA is associated with transcript destabilization. *ACS Chem Biol* 2020;**15**:132−9.
48. Zheng Q, Gan H, Yang F, Yao Y, Hao F, Hong L, et al. Cytoplasmic m^1A reader YTHDF3 inhibits trophoblast invasion by downregulation of m^1A-methylated IGF1R. *Cell Discov* 2020;**6**:12.
49. Woo HH, Chambers SK. Human ALKBH3-induced m^1A demethylation increases the CSF-1 mRNA stability in breast and ovarian cancer cells. *Biochim Biophys Acta Gene Regul Mech* 2019;**1862**:35−46.